Biogeosciences Discuss., 7, 1489–1527, 2010
www.biogeosciences-discuss.net/7/1489/2010/

Biogeosciences Discussions

This discussion paper is/has been under review for the journal Biogeosciences (BG).
Please refer to the corresponding final paper in BG if available.

An inverse analysis reveals limitations of the soil-CO_2 profile method to calculate CO_2 production for well-structured soils

B. Koehler[1,*], **E. Zehe**[2], **M. D. Corre**[1], **and E. Veldkamp**[1]

[1]Buesgen Institute – Soil Science of Tropical and Subtropical Ecosystems, University of Goettingen, Buesgenweg 2, 37077 Goettingen, Germany
[2]Institute of Water and Environment, Technische Universität München, Arcisstr. 21, 80333 Munich, Germany
[*]now at: Institute of Water and Environment, Technische Universität München, Arcisstr. 21, 80333 Munich, Germany

Received: 3 February 2010 – Accepted: 23 February 2010 – Published: 1 March 2010

Correspondence to: B. Koehler (koehlerbirgit@gmail.com)

Published by Copernicus Publications on behalf of the European Geosciences Union.

Abstract

Soil respiration is the second largest flux in the global carbon cycle, yet the underlying belowground process, carbon dioxide (CO_2) production, is not well understood because it can not be measured in the field. CO_2 production has frequently been calculated from the vertical CO_2 diffusive flux divergence, known as "soil-CO_2 profile method". This relatively simple method requires knowledge of soil CO_2 concentration profiles and soil diffusive properties. Application of the method in a tropical lowland forest soil in Panama gave inconsistent results when using diffusion coefficients (D) calculated based on relationships with soil porosity and moisture (empirical D). Our objective was to investigate whether these inconsistencies were caused by (1) the applied interpolation and solution methods, (2) uncertainties in describing the profile of D using empirical equations, or (3) the assumptions of the soil-CO_2 profile method. We show that the calculated CO_2 production strongly depended on the function used to interpolate between measured CO_2 concentrations. With an inverse analysis of the soil-CO_2 profile method we deduce which D would be required to explain the observed CO_2 concentrations, assuming the model assumptions are valid. In the top soil, this inverse D closely resembled the empirical D. In the deep soil, however, the inverse D increased sharply while the empirical D did not. This deviation between the empirical and inverse D disappeared upon conducting a constrained fit parameter optimization. A radon (Rn) mass balance model, in which diffusion was calculated based on the empirical or constrained inverse D, simulated the observed Rn profiles reasonably well. However, the CO_2 concentrations which corresponded to the constrained inverse D were too small compared to the measurements, and the inverse D gave depth-constant fluxes and hence zero production in the soil CO_2-profile method. We suggest that, in well-structured soils, a missing description of steady state CO_2 exchange fluxes across water-filled pores causes the soil-CO_2 profile method to fail. These fluxes are driven by the different diffusivities in inter- vs. intra-aggregate pores which create permanent CO_2 gradients if separated by a "diffusive water barrier". We conclude that the assumptions

BGD

7, 1489–1527, 2010

of the soil-CO_2 profile method are inaccurate for soils with pore networks which exhibit spatial separation between CO_2 production and diffusion out of the soil.

1 Introduction

Soil respiration, the efflux of CO_2 which is produced mainly by roots and decomposition of litter and organic matter, is the second largest flux in the global terrestrial carbon (C) cycle (IPCC, 2007). Because of its magnitude, even small changes in soil CO_2 production can affect atmospheric CO_2 concentrations and hence global warming. Despite this central role in the global C cycle, soil respiration remains among the least understood ecosystem C fluxes (Luo and Zhou, 2006).

CO_2 efflux at the soil-air interface is normally measured using chamber techniques while no direct field methods exist to measure soil CO_2 production at a specific soil depth. Mathematical models have been used to calculate soil CO_2 production with soil depth. In CO_2-production-transport models, microbial and root respiration are described on the process-scale (e.g. Šimůnek and Suarez, 1993; Fang and Moncrieff, 1999). An application of such models requires knowledge of several parameters for which often no information is available. A simpler approach is the "soil-CO_2 profile method" to calculate production rates from measured concentration profiles using gas diffusion modeling (DeJong and Schappert, 1972, 1978). This method has been used in several studies (Davidson and Trumbore, 1995; Gaudinski et al., 2000; Hirsch et al., 2002; Risk et al., 2002a, b, 2008; Davidson et al., 2004, 2006; Fierer et al., 2005; Jassal et al., 2005; Schwendenmann and Veldkamp, 2006; Hashimoto et al., 2007; Sotta et al., 2007). Recently, the method has also been applied in a slightly modified way to calculate soil nitrous oxide (N_2O) and methane (CH_4) turnover (Goldberg et al., 2008, 2010; Knorr et al., 2008a, b; Knorr and Blodau, 2009). The assumptions of the soil-CO_2 profile method are that 1) diffusion in the gas phase is the only relevant CO_2 transport pathway in soils, and 2) CO_2 concentrations in the soil gas and water phases are in steady state, i.e. changes over time are negligible. The CO_2 flux is described

BGD
7, 1489–1527, 2010

using Fick's first law of diffusion and, according to the model perception, the difference between the amount of CO_2 entering and leaving a soil layer is produced or consumed at that depth.

Application of the soil-CO_2 profile method requires accurate knowledge of the soil gas diffusion properties. As the calculated soil CO_2 production rates are directly proportional to D it is a highly sensitive model parameter, i.e. a doubling throughout the profile results in a doubling of the calculated CO_2 production. D is generally calculated choosing one of several functions that describe its relationship with soil properties like porosity and moisture (hereafter termed "empirical D"; e.g. Currie, 1961; Millington and Shearer, 1971; Moldrup et al., 2000). To determine the diffusion gradient, data on CO_2 concentrations in soil air are needed as further model input. In most of the above mentioned studies, measured CO_2 concentrations were linearly interpolated before numerically calculating CO_2 production using the finite difference method. In three studies, the measured CO_2 concentrations were interpolated using exponential (Gaudinski et al., 2000; Davidson et al., 2006) or quadratic (Jassal et al., 2005) functions, calculating CO_2 flux and production either analytically or numerically. In several studies, inconsistencies in depth-specific production rates and/or negative rates were encountered, which often led to the following simplifications: CO_2 production was added up over large depth intervals, and the CO_2 production of the top soil was estimated by subtracting the calculated subsoil CO_2 production from the measured soil CO_2 efflux. Explanations for the inconsistencies were an insufficient mathematical description of the relationship between D and the soil moisture content (DeJong and Schappert, 1972) and an inaccurate interpolation of CO_2 concentration profiles, especially in the top soil where "hot spots" of CO_2 production may occur (Davidson and Trumbore, 1995). Presently, despite their wide use, large uncertainties remain when using gas diffusivity models in soils (Davidson et al., 2006), which of course also introduces incertitude in the conclusions drawn from the model results.

We conducted a study in a tropical lowland forest in Panama in which we wanted to calculate depth-specific soil CO_2 production rates. When we applied the soil-CO_2

profile method on a 2-yr time series of soil CO_2 concentrations, we encountered similar inconsistencies as the ones described in earlier studies. The objective of the present study was to determine the cause for these inconsistencies. We tested the following hypotheses:

In the soil-CO_2 profile method

1. the procedures to interpolate between the measured CO_2 concentrations strongly influence the calculated CO_2 fluxes and production.
2. uncertainties in describing the depth distribution of D using soil characteristics cause inconsistencies in the resulting soil CO_2 production rates.
3. the perception of the processes governing soil CO_2 dynamics is inappropriate and/or incomplete.

To test these hypotheses we compared different methods for the CO_2 interpolation and solution of the soil-CO_2 profile method. Furthermore, we conducted an inverse analysis of the soil-CO_2 profile method to deduce which D would be required to explain the observed CO_2 concentrations, assuming the model assumptions are valid (hereafter termed "inverse" D). To test the accuracy of the determined empirical and inverse D, we used a radon (Rn) mass balance model. Finally, we verified the validity of the assumptions of the soil-CO_2 profile method based on its mathematical derivation and on the inverse modeling results.

2 Materials and methods

2.1 Measurements

2.1.1 Study area and experimental design

The study site is an old-growth, semi-deciduous tropical forest located at 25–61 m elevation on Gigante Peninsula (9°06′ N, 79°50′ W) which is part of the Barro Colorado

Nature Monument, Republic of Panamá. On nearby Barro Colorado Island, annual rainfall (1995–2007) averaged 2650±146 mm with a dry season from January to mid-May during which 297±40 mm of rainfall was recorded. The mean annual air temperature was 27.4±0.1 °C. Soils are derived from a basalt flow, have a heavy clay texture, and are classified as Endogleyic Cambisol in the lower parts of the landscape to Acric Nitisol in the upper parts of the landscape (FAO classification; alternatively Dystrudepts in USDA classification). Detailed soil characteristics and information on forest structure have been reported earlier (Koehler et al., 2009b; Corre et al., 2010).

We conducted our study in the three replicate control plots (untreated, 40 m×40 m each) of the "Gigante fertilization project" (described in details by Koehler et al., 2009b). The distance among these control plots was about 500 m. We measured soil CO_2 efflux, CO_2 concentrations in air (0.1 m above the soil surface) and in soil air at six depths down to 2 m, as well as soil moisture and temperature at the depths of air sampling (described below). These measurements were conducted in an approximately 6-weekly schedule from May 2006 to June 2008.

2.1.2 Soil CO_2 concentration profiles and soil CO_2 efflux measurements

In each of the three replicate plots, we established one permanent soil pit (1.6 m×0.8 m and 2.5 m deep). Stainless steel tubes (3.2 mm outer diameter) were installed horizontally into the pit walls at 0.05, 0.2, 0.4, 0.75, 1.25 and 2 m depth. In the top 1 m, tubes are 1 m long whereas the tubes at 1.25 m and 2 m depth are 1.8 m long to account for the pit wall effect on CO_2 concentrations (Schwendenmann et al., 2003). Tubes were perforated at one end and closed with a septum holder at the other end protruding from the pit wall. Soil air was sampled in evacuated glass containers (100 mL) closed with a teflon stopcock. Before sampling, 20 mL of air was discarded to remove the "dead volume" from the sampling tubes. Previous testing had shown that at least 300 mL could be withdrawn from a tube without changing CO_2 concentrations. Soil air samples were analyzed using a gas chromatograph (Shimadzu GC-14B, Columbia, MD, USA) equipped with an electron capture detector (Loftfield et al., 1997) which was calibrated

with three to four standard gases (360, 706, 1505, 5012 and 39 977 ppm CO_2, Deuste Steininger GmbH, Mühlhausen, Germany). Wet season soil-air sampling below 1 m depth was restricted because the groundwater table often rose above this depth. In one pit, CO_2 concentrations at 0.05 m were always larger than at 0.2 m depth. For the model calculations, these large values at 0.05 m depth were replaced by concentrations interpolated from the other two pits. Surface soil CO_2 effluxes were measured by sampling air from four vented static chambers per plot with subsequent gas chromatographic analysis, and were calculated based on a quadratic or linear regression model using the Akaike Information Criterion as statistical decision tool. A detailed method description of the flux measurements was provided by Koehler et al. (2009a).

2.1.3 Soil ^{222}Rn concentration profiles

We measured ^{222}Rn concentration profiles in soil air, twice at the end of the dry season 2006/07, and twice at the height of the wet season 2007. In each of the three soil pits, soil air was sampled in pre-evacuated scintillation flasks (Lucas cells 110A and 300A, Pylon Electronics, Ontario, Ottawa, Canada) in which alpha particle emission from radioactive decay was detected using a portable radiation monitor (AB-5, Pylon Electronics). The counting efficiencies of the scintillation flasks, determined after transferring a known amount of ^{222}Rn using a flow through Rn source (Pylon Model RN-1025-20, Pylon Electronics), ranged from 71 to 82%. Before each use, the background activity of the flasks was determined after repeatedly evacuating and flushing them with nitrogen gas followed by a time span of at least 24 h. Mean background was 0.88±0.04 counts per minute (cpm). During sampling, the air was filtered for ambient alpha particles (PTFE-membrane 0.45 µm, Minisart SRP25, Sartorius, Goettingen, Germany) and dried using a $CaCl_2$-column (30 mL). Sampling proceeded from 0.05 m (smallest concentrations) to 2 m depth (largest concentrations). The sampling system was repeatedly flushed with ambient air in between samplings. A delay of at least 3.5 h permitted the establishment of the radioactive equilibrium of ^{218}Po and ^{214}Po after which alpha decays were counted for six 5-min intervals within 24 h. Mean background

activity was subtracted from mean sample activity. Activities (cpm) were corrected for the counting efficiency of the scintillation flask, for decay during the counting interval, and for decay during the interval between sampling and measurement (Pylon Electronics, 1989), and were converted to Bq m^{-3}.

2.1.4 Laboratory measurements of soil ^{222}Rn production

During pit establishment, soil samples (~150 g dry weight) were taken from the same depths where air sampling tubes were subsequently installed. The soil was air-dried and incubated for 12–18 days in air-tight jars (1700 mL) to permit ^{222}Rn to build up and approach equilibrium with the parent isotope ^{226}Ra. Between 89 and 96% of the equilibrium production rate is reached during this incubation time. Rn concentrations (Bq m^{-3}) were determined from duplicate air samples taken from the incubation jars, as described above. Afterwards, the same soil samples were adjusted to soil moisture contents representative for wet season conditions, and the incubation and Rn determination were repeated. The equilibrium Rn production rates P (Bq kg^{-1}) were calculated as:

$$P = \frac{\mathrm{Rn} \cdot V_g}{m} f \quad (1)$$

where V_g is the air volume in the incubation jar (m^{-3}), m is the dry soil weight (kg) and f is the conversion factor to equilibrium production rate ($f = 1–0.5^n$ with n=number of ^{222}Rn half lives passed during the incubation time). V_g is the difference between the jar volume and the soil-occupied volume as well as, for the wet soil incubations, the volume of added water.

2.1.5 Additional measurements in the soil pits

Soil bulk density was determined from two undisturbed 250 cm^3 soil cores (Blake and Hartge, 1986) sampled during pit establishment at the six depths where air sampling

tubes were subsequently installed. Soil water characteristic curves (laboratory pF curves) were determined on one undisturbed 250 cm^3 soil core per sampling depth from two soil pits, with a suction membrane in the lower suction range (0–330 hPa) and a pressure membrane device in the higher suction range (1000–15 000 hPa). Thermocouple T-probes (Omega Engineering, Deckenpfronn, Germany) were attached at the perforated end of the air sampling tubes, and water content probes (Campbell Scientific CS616, Logan, Utah) were installed next to them. Some clay types (our soils have a heavy clay texture with up to 70% clay; Koehler et al., 2009b) can attenuate the CS616 probe response as described by the manufacturers standard calibration and, consequently, a soil specific calibration is required (Campbell Scientific, 2002–2006). To establish this soil specific sensor calibration, we used four undisturbed 4000 cm^3 soil samples taken during the establishment of one of the pits. Soil samples were first water-saturated and during subsequent drying (at 24 °C in the laboratory) both sensor output and gravimetric soil moisture were determined daily for two weeks (as described in Veldkamp and O'Brien, 2000). The CS616 sensors are temperature dependent and signals were converted to 20 °C using the manufacturer's formula. Our soil specific calibration function was VWC ($cm^3\,cm^{-3}$)$=-0.002\,x^2+0.149\,x-2.101$ ($R^2=0.87$, $n=58$, $P<0.001$) where VWC is the volumetric water content and x is the sensor period signal (ms). This calibration achieved a root mean squared error (RMSE) of 0.049 compared to a RMSE of 0.135 if the manufacturer's standard calibration function was applied. We used a quadratic calibration function instead of a 3-phase-model (as applied by Veldkamp and O'Brien, 2000) because it reached a better performance.

2.1.6 Empirical calculation of gas diffusion coefficients *D*

To calculate D for the depths of air sampling, we used a semi-empirical cut- and random-rejoin-type model for aggregated porous media (Millington and Shearer, 1971). The required input parameters are D in free air (0.139 $cm^2\,s^{-1}$ for CO_2 (Pritchard and Currie, 1982) and 0.11 $cm^2\,s^{-1}$ for ^{222}Rn (Sasaki et al., 2006) at $T_0=273.2$ K and $P_0=1013$ hPa), the total inter- and intra-aggregate pore space (ε_{inter} and ε_{intra},

respectively) and the water distribution between them. Soil total porosity (θ_s) was calculated from bulk density assuming a particle density of 2.65 g cm^{-3} for mineral soil (Linn and Doran, 1984). Considering that inter-aggregate pores drain quickly, we calculated ε_{inter} as the difference between water content at saturation and at field capacity (Radulovich et al., 1989), which we defined as the water content remaining after applying a suction of 10 kPa to the water-saturated soil (Hillel, 1998). ε_{intra} is the difference between θ_s and ε_{inter}. To estimate the water distribution between the pore classes we assumed that water can only occur in ε_{inter} if ε_{intra} is water saturated, and that ε_{inter} is completely air-filled if the VWC is below field capacity (Collin and Rasmuson, 1988). To account for the temperature dependence of diffusion, we multiplied D with the term $(T/T_0)^n$ where T is the soil temperature during air sampling (K), T_0 is 273.2 K and n is 1.75 for CO_2 (Campbell, 1985).

2.2 Model approach and calculation methods

2.2.1 The soil-CO_2 profile method

In the "soil-CO_2 profile method", soil CO_2 production is calculated from the vertical divergence of the CO_2 diffusive flux in the gas phase (DeJong and Schappert, 1972):

$$S_t = -\frac{\partial}{\partial z}\left(D_g \frac{\partial C_g}{\partial z}\right) \quad (2)$$

where S_t is the total CO_2 production in gas and water phases (ng cm^{-3} s^{-1}), z is depth (cm), D_g is the effective diffusion coefficient in the gas phase (cm^2 s^{-1}) and C_g is the CO_2 concentration in the gas phase (ng cm^{-3}). This is a simplification of the total soil CO_2 mass balance equation in the gas and water phase (please see Appendix A for a detailed derivation) that is based on four assumptions: 1) CO_2 is in steady state in gas and water phases (which implicitly contains the assumption that CO_2 equilibration between the phases establishes instantaneously), 2) convective CO_2 transport can

be neglected, and diffusion in the water phase can be neglected, 3) the system is horizontally homogeneous, and 4) there are no relevant CO_2 sinks in soils (S_t should always be >0). Based on assumption 4 and in concert with earlier studies we call S_t "CO_2 production" from now on, though this term may become negative.

2.2.2 Parameterization of the soil-CO_2 profile method

According to the soil-CO_2 profile method (Eq. 2), the CO_2 production profile can be calculated if the derivatives of the CO_2 concentration profile and the profile of D are known. To achieve the first requirement, we used the asymmetric sigmoidal Gompertz function (Richards, 1959) to approximate our observed CO_2 distribution, i.e. to interpolate the measured CO_2 concentrations on a regular (0.05 m) vertical grid (Fig. 1a):

$$C_g = ae^{be^{cz}} \tag{3}$$

Estimates for the parameters a, b and c were obtained using non-linear least square fitting to the measured CO_2 concentration profiles. The first derivative describes the concentration gradient driving gaseous diffusion (Fig. 1b):

$$\frac{\partial C_g}{\partial z} = abce^{cz+be^{cz}} \tag{4}$$

The second derivative is the curvature of the concentration profile (Fig. 1c). In case of a constant D it would be the proportional to S_t:

$$\frac{\partial^2 C_g}{\partial z^2} = abc^2e^{cz+be^{cz}}(1+be^{cz}) \tag{5}$$

To parameterize D (second requirement), we 1) used the empirical function by Millington and Shearer (1971) as described in Sect. 2.1.6 and 2) set up an inverse analysis of the soil-CO_2 profile method to obtain an equation to calculate D, making use of the

model assumptions (see Sect. 2.2.1), and based on the derivatives of the function fitted to the observed gas profile (Eqs. 4 and 5). In the following, we explain this inverse analysis starting from Eq. (2), which can also be written as:

$$S_t = -\frac{\partial D_g}{\partial z}\frac{\partial C_g}{\partial z} - D_g\frac{\partial^2 C_g}{\partial z^2} \quad (6)$$

According to assumption 4, S_T must be greater than zero:

$$-\frac{\partial D_g}{\partial z}\frac{\partial C_g}{\partial z} - D_g\frac{\partial^2 C_g}{\partial z^2} > 0 \quad (7)$$

Equation (7) can be rearranged such that the unknown terms are on the left-hand side and the known terms are on the right-hand side:

$$-\frac{\partial D_g}{\partial z}\frac{1}{D_g} > \frac{\frac{\partial^2 C_g}{\partial z^2}}{\frac{\partial C_g}{\partial z}} \quad (8)$$

Inserting Eqs. (4) and (5) in the right-hand side of Eq. (8) gives:

$$-\frac{\partial D_g}{\partial z}\frac{1}{D_g} > c + bce^{cz} \quad (9)$$

Definite integration of the left hand side of Eq. (9) from depth z to the surface (z=0) gives:

$$\int_0^z -\frac{\partial D_g}{\partial z}\frac{1}{D_g}\partial z = -\ln\left(\frac{D_{g_z}}{D_0}\right) \quad (10)$$

Analogous, indefinite integration of the right-hand side of Eq. (9) gives:

$$\int c + bce^{cz}\,dz = cz + be^{cz} + const \quad (11)$$

where *const* is an integration constant. Based on Eqs. (10) and (11) follows:

$$-\ln\left(\frac{D_{g_z}}{D_0}\right) > cz + be^{cz} + const \tag{12}$$

By taking the exponential of Eq. (12) we get our target function, an equation to calculate D as function of z:

$$D_{g_z} < D_0 e^{-cz-be^{cz}-const} \tag{13}$$

Thereby, *const* is given as:

$$const < \ln\frac{D_0}{D_{g_z}} - cz - be^{cz} \tag{14}$$

In the simulations, we converted *const* to the correct scale by multiplying our inverse "maximal" profile of D (Eq. 13) with the factor "empirical D/inverse D" at all depths. Consequently, the inverse D at the upper boundary (z=0) becomes equal to the empirical D (Millington and Shearer, 1971) calculated for 0–0.05 m depth.

In a next step, we fitted the sigmoidal function (Eq. 3) to the measured CO_2 profiles such that D must always increase monotonically with z, i.e. increase with decreasing soil depth ($\partial D/\partial z > 0$; see Sect. 3.2). The first derivative of Eq. (13) reads:

$$\frac{\partial D_{g_z}}{\partial z} < D_0 e^{-cz-be^{cz}-const}(-c - cbe^{cz}) \tag{15}$$

From Eq. (15) it can be recognized that the constraint $\partial D/\partial z > 0$ is fulfilled when the term in brackets becomes positive, thus:

$$-c - cbe^{cz} > 0 \tag{16}$$

We used the method of simulated annealing to conduct the constrained parameter optimization (Kirkpatrick et al., 1983).

2.2.3 Implementations of the soil-CO_2 profile method

To compare the results of our inverse parameterization with the results achieved with the usual solution methods of the soil-CO_2 profile method, we conducted the following calculations: First, we determined CO_2 fluxes (Fick's first law of diffusion) and production using the empirical D and a) the finite difference method after linear interpolation between measured CO_2 concentrations on a regular vertical grid (DeJong and Schappert, 1972; Davidson and Trumbore, 1995), b) the analytical solution of an exponential interpolation function (Gaudinski et al., 2000), and c) the analytical solution of our chosen sigmoidal interpolation function (Eq. 3). Secondly, we used the inverse D to determine CO_2 fluxes (Fick's first law of diffusion) and production (inserting Eqs. 4, 5, 13 and 15 in Eq. 6). Mass-based CO_2 production rates (per soil volume) were converted to area-based production rates by multiplying with the depth of the soil layer (dz=0.05 m). The sum of all area-based production rates is the mineral soil CO_2 production of the total profile, or the modeled soil surface CO_2 efflux. We only calculated CO_2 production for profiles where we could measure CO_2 concentrations down to at least 1.25 m depth. All calculations were conducted using MATLAB® 7.0.1 (The MathWorks, Natick, MA, USA, 2004).

2.2.4 Rn mass balance model

We set up a one-dimensional Rn mass balance model which considers production, decay in water and gas phases, gaseous diffusion and exchange between the gas and water phase assuming instantaneous equilibration (Davidson and Trumbore, 1995; Schwendenmann and Veldkamp, 2006). We used this model to test the validity of D by comparing simulated steady state with measured profiles of Rn concentrations. The Rn production rates were adjusted to the soil moisture during Rn sampling based on the production rates measured from dry and wet soil. We established Dirichlet boundary conditions, specifying the Rn concentration measured at 0.05 as upper and at 2 m depth as lower boundary condition. For the other depths, the initial Rn concentration

in soil air was calculated depending on the measured soil water content. The model was solved with MATLAB® 7.0.1 (The MathWorks, 2004) using an explicit numerical method on a 0.05 m vertical grid until steady state was established.

2.2.5 Statistical analyses and calculations

If data sets were rightly skewed, we applied either a square-root or a logarithmic transformation before analysis. If data sets were left-skewed, a quadratic or cubic transformation was applied before analysis. Linear mixed effects models (on plot means) were used to test the time series of the response variables for a fixed effect of seasons (for VWC, soil temperature, air-filled porosities and soil CO_2 efflux) or calculation methods (for D), with the spatial replication nested in time as random effects. The models were specified as explained by Koehler et al. (2009b) and the significance of the fixed effect was assessed using analysis of variance (Crawley, 2002). For soil porosities and Rn production rates, we assessed differences between seasons and incubations (dry vs. wet) using independent t tests. Effects were considered significant if P value ≤ 0.05. We used the root mean squared error (RMSE) as criterion for the goodness of fit of the interpolation functions to the measured CO_2 concentrations. Mean values in the text are given with ±1 standard error. Statistical analyses were conducted using *R*2.9.0 (R Development Core Team, 2009).

3 Results

3.1 Volumetric water content, temperatures, ^{222}Rn and CO_2 concentrations down to 2 m soil depth

The volumetric water content (VWC) increased with soil depth and was smaller during dry than wet season at all sampling depths (all $P < 0.001$). Mean soil temperatures ranged between 24.9±0.1 and 25.2±0.1 °C, and varied seasonally by 2.4 °C at

0.05 m depth, by 2.1 °C at 0.2 m depth, and by 1.3 to 1.7 °C at deeper depths (data not shown). ^{222}Rn concentrations increased with soil depth and exhibited a sigmoidal profile shape both during dry and wet season (Fig. 2). Soil CO_2 concentrations averaged 830±35 ppm at 0.1 m above the soil surface, and increased with soil depth. The strongest increase occurred down to 0.2 m depth where concentrations averaged 0.31±0.02% during dry season and 0.65±0.06% during wet season. At 2 m depth, CO_2 concentrations were up to 55 times larger than the concentration above the soil surface, with an annual mean of 4.22±0.32%. CO_2 concentrations displayed a pronounced seasonality especially in the top 0.75 m soil, with largest concentrations at the end of wet season and smallest concentrations at the end of dry season (Fig. 3).

3.2 Soil porosity and empirical diffusion coefficients

In general, both total and inter-aggregate soil porosity decreased with soil depth. Also air-filled porosity decreased with soil depth, with the sharpest decline in the top 0.4 m soil, and smaller values during wet than dry season at all sampling depths (all $P < 0.013$; Table 1). The empirical D resembled this depth pattern of air-filled porosities (Fig. 4a and b). It was smaller during wet than dry season down to 1.25 m depth (all $P < 0.037$) but did not differ between seasons at 2 m depth.

3.3 Soil ^{222}Rn production rates and model simulated steady state ^{222}Rn concentrations

The Rn production rates decreased with soil depth, and were larger but statistically undistinguishable from the wet compared to the dry soil (Table 1). Using the Rn production rates and the empirical D in the Rn mass balance model, the simulated steady state concentrations were larger than measured during dry season (Fig. 2a), but matched the measured concentrations well during wet season (Fig. 2b). A sensitivity analysis shows that the steady state model solution was more sensitive to changes in the Rn production rates than in D (inset in Fig. 2a).

3.4 CO_2 fluxes and production rates calculated with the empirical *D* and different implementations of the soil-CO_2 profile method

The best fit to the measured CO_2 concentrations was achieved with a sigmoidal function (RMSE=0.14±0.04). An exponential function gave a worse fit (RMSE=0.22±0.04; Fig. 4c and d). When using the empirical *D* and the sigmoidal interpolation function in the soil-CO_2 profile method, the resulting CO_2 flux increased slightly with decreasing soil depth. In contrast, when using the exponential interpolation function, the flux increased strongly towards the surface, which gave a three-fold larger mean surface flux (Fig. 5a). The simulated CO_2 production based on a sigmoidal function was close to zero, became slightly negative at some depths and displayed a peak in the top soil. The exponential function led to very small CO_2 production rates below a depth of 0.75 m and a strong increase towards the soil surface (Fig. 5b). We do not present the results based on the finite difference method after linear interpolation between the measured CO_2 concentrations for reasons discussed in Sect. 4.1.

The measured soil CO_2 effluxes averaged 198.10±9.18 mg C $m^{-2} h^{-1}$ and were smaller during dry season (113.38±13.84 mg C $m^{-2} h^{-1}$) than wet season (212.60±6.97 mg C $m^{-2} h^{-1}$, $P < 0.001$). All of the applied solution methods displayed seasonality in the total soil CO_2 production (i.e. the modeled soil CO_2 efflux). However, use of the empirical *D* with the sigmoidal function resulted in production rates that were too small compared to the measured effluxes. Use of the exponential function increased the calculated production rates three-fold, over- and underestimating at times the measured effluxes (Fig. 6). When using the empirical *D* and the finite difference method after linear interpolation between the measured CO_2 concentrations the CO_2 production rates increased with the resolution of the interpolation grid (not shown).

BGD
7, 1489–1527, 2010

3.5 CO_2 fluxes and production rates calculated with the inverse D in the soil-CO_2 profile method

When we calculated the inverse D based on non-linear least-square fitting of the sigmoidal function to the measured CO_2 profile, it closely resembled the empirical D in the top ~0.75 m soil during dry season and in the top ~0.4 m soil during wet season. In contrast to the empirical D, the inverse D increased sharply below these depths. After adding the constraint that D must decrease monotonically with soil depth (Eq. 16), the inverse D resembled the empirical D throughout the profile but was slightly larger ($P < 0.001$ at all sampling depths, Fig. 4a and b). This constrained inverse D gave a similar result as the empirical D when used in the Rn mass balance model (Fig. 2). However, it did not reproduce the measured soil CO_2 concentrations, which were underestimated (RMSE=0.46±0.10; Fig. 4c and d).

Using the inverse D (Eq. 13) and the corresponding interpolated CO_2 concentrations (Eq. 3) in the soil-CO_2 profile method, the resulting CO_2 flux was constant with depth (Fig. 5a), which means that the CO_2 production term was zero at all depths. With Eq. (6) it can be shown that this is true in general: D is positive at all depths (Fig. 4a and b). The first derivative of a sigmoidal function is negative (<0) at all depths (Fig. 1b) while its second derivative is positive in the top and negative in the deep soil (Fig. 1c). Thus, to get positive CO_2 production terms, also $\delta D/\delta z$ must be positive at all depths which is sensible concerning that the empirical D indeed decreased monotonically with depth (Fig. 4a and b). In the inverse analysis, this condition was not immediately fulfilled but the solution can be forced to meet it by implying the parameter constraint of Eq. (6) (Fig. 4a and b). In the top soil, a further requirement for positive CO_2-production terms is that:

$$\left| \frac{\partial D_g}{\partial z} \frac{\partial C_g}{\partial z} \right| > \left| D_g \frac{\partial^2 C_g}{\partial z^2} \right| . \quad (17)$$

Inserting the respective terms (Eqs. 4, 5, 13 and 15) shows that the absolute values of

the left and right-hand expressions are the same:

$$\frac{\left|-c-cbe^{cz}\right|}{\left|c+cbe^{cz}\right|}=1 \tag{18}$$

This formally explains why the condition of Eq. (17) could not be fulfilled, and why the inversely modeled CO_2 production was zero at all depths (Fig. 5b). We conducted a similar inverse analysis to calculate profiles of D and S with an exponential function (equivalent to Eqs. 9 to 13 with $C_g = a\,(1-e^{-bz})$, not shown). The first derivative of the resulting profile of D was always <0 and consequently the CO_2 production term was negative at all depths. Also in this case it was impossible to obtain a solution where $S>0$.

4 Discussion

4.1 Influence of the function to interpolate between the measured CO_2 concentrations on the calculated CO_2 production

Vertical interpolation between measured CO_2 concentrations is necessary to apply the soil-CO_2 profile method with a fine depth resolution. In several studies the CO_2 concentrations were linearly interpolated and the concentration gradient driving diffusion ($\delta C/\delta z$) was calculated numerically using the finite difference method. Finite differences, however, may only be used to approximate the derivatives of continuous functions, whereas in these studies the method was applied on a set of linear functions which changed at the measurement depths. As $\delta C/\delta z$ remains undefined at those depths the calculated CO_2 production rates depend on the depth resolution of the interpolation grid. This influence was already observed by DeJong et al. (1978) who reported that "the discrepancies between the static chamber and soil-CO_2 profile estimates decreased as the calculations for the latter method were based on thicker soil layers". This is, however, a mathematical artifact and we conclude that the combination

of linear interpolation with finite differences leads to artificial results. If the soil-CO_2 profile method is applied, the interpolation between measured CO_2 concentrations could only be conducted using continuous and differentiable functions.

Selection of an adequate interpolation function is critical because in the soil-CO_2 profile method the calculated flux will only be accurate if the concentration gradient is described correctly. In our case, the observed steady state soil gas profile could be best described using a sigmoidal function (Figs. 2, 4c and d). This functional type has not been used before but for several other studies the shape of soil Rn and CO_2 profiles suggests that it would have resulted in good fits as well (e.g. Dörr and Münnich, 1990; Elberling, 2003; Jassal et al., 2004; Fierer et al., 2005; Schwendenmann and Veldkamp, 2006). In our study, the calculated CO_2 production was unrealistically small compared to the measured CO_2 effluxes (Fig. 6). Although the use of an exponential interpolation would lead to more "ecologically reasonable" results (both flux and production profiles increase towards the surface, Fig. 5), these profiles are largely caused by the monotonically increasing negative first and second derivatives of exponential functions. In our study, an exponential function (as was used in Gaudinski et al., 2000, and Davidson et al., 2006) did not match the observed steady state Rn profile (Fig. 2), gave a worse fit than the sigmoidal function (Fig. 5) and did not reproduce the measured CO_2 fluxes (Fig. 6). Replacing the sigmoidal with an exponential interpolation function, however, increased the calculated areal production rates on average threefold which puts the forecasting power of the soil-CO_2 profile method into question. Using the soil-CO_2 profile method with a sigmoidal function, which best describes our sites' steady state soil gas distribution, yielded inconsistencies similar to the ones reported in earlier applications.

4.2 Influence of uncertainties in the depth distribution of *D*

As, in the soil-CO_2 profile method, CO_2 production is directly proportional to D the choice of a function to describe it has been identified as a major source of uncertainty in earlier studies. For example, when using two different models to calculate D

for the same site, the calculated organic horizon CO_2 production differed by a factor of two (Gaudinski et al., 2000; Davidson et al., 2006). Furthermore, an empirically calculated *D* yielded over- or under-predictions of up to two orders of magnitude compared to values measured in situ (Risk et al., 2008). The Millington and Shearer (1971) model to calculate *D* based on soil properties generally performs well in aggregated clay soils (Collin and Rasmuson, 1988), and the resulting empirical *D* of our study was comparable to those calculated for tropical forest Oxisol soils in Brazil (Davidson and Trumbore, 1995) and Costa Rica (Schwendenmann and Veldkamp, 2006). The results from the Rn mass balance model suggest that our empirical *D* was adequate during wet season conditions (Fig. 2b). Although the Rn concentrations were overestimated in the dry-season simulation (Fig. 2a), the overall results were superior to alternative empirical models to calculate *D*. The Rn mass balance model was sensitive to the Rn production rates (inset in Fig. 2a). These were measured in laboratory incubations with disturbed soil samples, and soil moisture during the incubations was not identical to conditions encountered during the field campaigns when Rn concentrations were measured. Therefore, the experimentally derived Rn production rates might not describe the in-situ conditions sufficiently well. We conclude from the Rn mass balance simulations and the model sensitivity analysis that the empirical *D* was reasonably well constrained.

We tested this conclusion independently by comparing the empirical *D* with inversely modeled *D*. The pattern of the air-filled porosity, which determines the distribution of *D*, indicates that the observed increase of the unconstrained inverse *D* at deeper depths was unrealistic (Table 1). The fact that the additional constraint gave an inverse *D* which matched the empirical *D* well also in the deep soil (Fig. 4a and b) supports the assumption that the latter is accurate. However, the CO_2 concentrations which corresponded with these constrained inverse *D* were too small compared to the measurements (Fig. 4c and d), and resulted in zero CO_2 production in the soil-CO_2 profile method (Fig. 5b). We conclude from the inverse analysis that our measured CO_2 concentration profiles can not be explained when gas diffusion is the only described model

process, but that an additional CO_2 sink exists, which is missing in the mathematical description. As the inverse analysis of an exponential function gave inconsistent results as well this conclusion is independent of the function we chose to approximate the CO_2 concentration profile.

4.3 Processes governing soil CO_2 dynamics

The key assumptions of the soil-CO_2 profile method are that convective soil CO_2 transport in water is negligible, and that CO_2 equilibration between air and water phase occurs instantaneously (Sect. 2.2.1, Appendix A). The limiting factor here is the diffusive velocity of CO_2 in water (D_w), which is 1.94×10^{-5} cm^2 s^{-1} at 25 °C (Tse and Sandall, 1979). For the dry season, evaporative water losses, which cause a continuous increase in the air-filled porosity and consequently a decrease in CO_2 concentrations, might violate the steady state assumption. However, the observed soil moisture reduction of ~0.2 cm^3 cm^{-3} at 0.05 m depth (not shown) results in a decrease in CO_2 concentrations of only ~5% from December to April. At deeper depths, where drying was less and CO_2 concentrations were larger, this effect is even smaller. For the wet season, we estimated the water flow velocity at which the time scale of convection τ_A approaches the characteristic diffusion time τ_D of a CO_2 molecule through a water-filled circular pore. τ_D is ~10^2 s for a pore diameter of 1 mm (upper end of the size range of intra-aggregate pores; Hillel, 1998), thus $\tau_A$would need to surpass 10^{-5} m s^{-1}. Natural soils usually contain a network of non-capillary macropores, formed e.g. by shrinking and swelling of clay soils, roots or the soil fauna (Beven and Germann, 1982). Preferential flow velocity in macropores, including inter-aggregate pores (ε_{inter}), can increase to the order of 10^{-2} to 10^{-3} m s^{-1} for short time periods during heavy rainfall (Beven and Germann, 1982; Zehe and Flühler, 2001; Zehe and Sivapalan, 2009). At our site, the average air-filled porosity exceeded ε_{inter} even during wet season (Table 1), which makes the occurrence of such rapid, event-based water transport likely (Blume et al., 2008). In contrast, the velocity required to disturb the diffusive CO_2 equilibration

between gas and water phases is probably never reached in the clay soil matrix, given its small hydraulic conductivity. Thus, except for short periods during heavy storms, both key assumptions of the soil-CO_2 profile method are fulfilled at our site.

We suspect that the network of inter-aggregate pores is important to explain the observed inconsistencies when applying the soil-CO_2 profile method. This network is usually fairly well connected in aggregated soils (Beven and Germann, 1982; see e.g. Fig. 7a) and, because of faster "preferential" diffusion, better aerated than the intra-aggregate air-filled pores (α_{intra}) (Hillel, 1998). This results in CO_2 concentrations in the inter-aggregate air-filled pores (α_{inter}) which are considerably smaller than in α_{intra}. If soil air in inter- and intra-aggregate pores is separated by a water film, the equilibrium CO_2 concentration for the water phase is different at the respective interfaces. This yields a CO_2 gradient across the water film which results in diffusive CO_2 leakage into α_{inter} (Fig. 7b). As the diffusion in α_{intra} and water is much slower than in α_{inter}, these gradients can not be depleted during steady state conditions. At deeper depths, ε_{inter} and D are smaller resulting in a stronger CO_2 accumulation in the intra-aggregate pores. This explains why, according to the results of our inverse analysis, the largest CO_2 sink was needed in the subsoil, and why the deviation between empirical and unconstrained inverse D was more pronounced during wet than dry season (Fig. 4a and b). The same steady state exchange process occurs close to the soil surface where soil water has interfaces with the differing CO_2 concentrations in α_{intra}, α_{inter} and free air. Similarly, separation between gas production and transport by the water phase has been suggested as explanation for failed attempts to calculate soil N_2O fluxes with the so-called gradient method (Heincke and Kaupenjohann, 1999). Support for our theory comes from the Rn mass balance simulations which, in contrast to the soil-CO_2 profile method, include Rn exchange between soil gas and water phase. The Rn simulations captured the shape of the measured profiles, which suggests that, despite the poor solubility of Rn (Sander, 1999), inclusion of soil water and the coupling between the water and gas phases are relevant during steady state (Fig. 2). For CO_2, which is much more soluble, this will even be more important.

4.4 Implications of this study for the mathematical modeling of pedogenic trace gas dynamics

The soil-CO_2 profile method has been widely applied because of its relative simplicity. However, inconsistencies have been reported in many of the studies, and also by the authors who developed the method. We found evidence that, for well-structured soils, the inconsistencies may not mainly be caused by inaccurate interpolation or parameterization but more likely by 1) the omission of soil water in the CO_2 mass balance setup, and 2) the theory to treat soil gas diffusion as homogeneous process. Inclusion of water is required to describe the steady state CO_2 exchange between the soil gas and water phases, which is caused by persistent CO_2 gradients between inter- and intra-aggregate air-filled pores if separated by water. A two-domain macropore/matrix model (similar to approaches used to model soil water flow; Beven and Germann, 1982; Šimůnek et al., 2003) may be required to account for the different diffusional characteristics of the pore systems, and to describe the interaction between them. As our inverse analysis was only based on the vertical CO_2 distribution and the assumptions of the soil-CO_2 profile method, this conclusion is independent from the ecosystem where we conducted our study. Moreover, it is not only valid for CO_2 but for pedogenic trace gases in general. Consequently, we can only improve our understanding of soil trace gas dynamics by using process-based production/consumption-transport models, which consider the mass balance in both gas and water phases, and possibly dual-porosity transport.

Appendix A

The mathematical derivation of the soil-CO_2 profile method is based on the mass balance of CO_2 in soils, which can be modeled as:

$$\frac{\partial C_t}{\partial t} = \frac{\partial \theta C_w}{\partial t} + \frac{\partial (\theta s - \theta) C_g}{\partial t} = -\frac{\partial}{\partial z}\left(q_g C_g + q_w C_w - D_g \frac{\partial C_g}{\partial z} - D_w \frac{\partial C_w}{\partial z}\right) + S \quad \text{(A1)}$$

where C_t is the total concentration of CO_2 in the gas (C_g) and water phases (C_w; ng cm^{-3}), t is time (s), θ is the volumetric soil water content (cm^3 cm^{-3}), z is depth (cm), θ_s is total soil porosity (cm^3 cm^{-3}), q is the mass flux (cm s^{-1}) of water or air, D is the effective diffusion coefficient (cm^2 s^{-1}), and S are CO_2 sources and sinks (ng cm^{-3} s^{-1}). Assuming horizontal homogeneity, the diffusive fluxes are expressed according to Fick's first law of diffusion in one spatial dimension. Positive fluxes are defined as upward (towards the atmosphere), and negative fluxes as downward (towards deeper soil). The equilibrium concentrations of CO_2 in the water and gas phase can be described according to Henry's law:

$$\frac{C_w}{C_g} = k_H := \frac{k_1}{k_2} \quad \text{(A2)}$$

where k_H is Henry's law constant, and k_1 and k_2 are the dissolution and volatilization rate coefficients, respectively. Assuming absence of CO_2 sinks in soils (hence S is CO_2 production) and neglecting convective transport and diffusion in the water phase, the mass balances in the gas and water phases are simplified to:

$$\frac{\partial (\theta s - \theta) C_g}{\partial t} = -\frac{\partial}{\partial z}\left(-D_g \frac{\partial C_g}{\partial z}\right) + S_g - k_1 C_g + k_2 C_w \quad \text{(A3)}$$

$$\frac{\partial \theta C_w}{\partial t} = S_w + k_1 C_g - k_2 C_w \quad \text{(A4)}$$

BGD
7, 1489–1527, 2010

where S_g and S_w denote the fractions of CO_2 production which first occur in the gas and water phases, respectively. It is assumed that diffusive CO_2 exchange across the air-water interfaces and subsequent mixing is much faster than temporal changes in CO_2 concentration, and consequently the equilibrium establishes instantaneously (i.e. CO_2 in the water phase is in steady state). Equation (A4) then reduces to a diagnostic equation:

$$k_2 C_w = S_w + k_1 C_g \tag{A5}$$

Insertion of Eq. (A5) into Eq. (A3) allows elimination of C_w:

$$\frac{\partial(\theta s - \theta)C_g}{\partial t} = -\frac{\partial}{\partial z}\left(-D_g \frac{\partial C_g}{\partial z}\right) + S_g + S_w \tag{A6}$$

Finally, assuming that the CO_2 concentrations in the air phase are in steady state, one obtains:

$$S_t = S_g + S_w = -\frac{\partial}{\partial z}\left(D_g \frac{\partial C_g}{\partial z}\right) \tag{A7}$$

This equation is called "soil-CO_2 profile method" (DeJong and Schappert, 1972, 1978).

Acknowledgements. We thank S. Joseph Wright for hosting the experimental part of our study in his site, and for discussion and support; Rodolfo Rojas, Carlos Sanchez and Olivier Gonzalez for their dedicated assistance during field measurements; Norman Loftfield and Luitgard Schwendenmann for their advice concerning gas analytic procedures; Michael Gründel for calibration of Lucas cells in the ISOLAB at the University of Goettingen; Hans-Jörg Vogel for providing us with the soil X-ray CT image; Ulrike Talkner and Katrin Wolf for helpful discussions; the Smithsonian Tropical Research Institute for excellent logistical and technical support. B. Koehler acknowledges funding by a post doctoral grant from the "Technische Universität München", and from Harald Horn at the Institute of Water Quality Control; the experimental part of this study was funded by the grant of the Robert Bosch Foundation to M. D. Corre (independent research group NITROF).

GEORG-AUGUST-UNIVERSITÄT
GÖTTINGEN

This Open Access Publication is funded by the University of Göttingen.

References

Beven, K. J. and Germann, P. F.: Macropores and water flow in soils, Water Resour. Res., 18, 1311–1325, 1982.

Blake, G. R. and Hartge, K. H.: Bulk density, in: Methods of soil analysis, part 1. Physical and mineralogical methods, edited by: Klute, A., Agronomy Monograph, Soil Sci. Soc. Am., Madison, Wisconsin, USA, 12, 1986.

Blume, T., Zehe, E., and Bronstert, A.: Investigation of runoff generation in a pristine, poorly gauged catchment in the Chilean Andes II: Qualitative and quantitative use of tracers at three spatial scales, Hydrol. Processes, 22, 3676–3688, 2008.

Campbell, G. S.: Soil physics with BASIC, transport models for soil-plant systems, Developments in Soil Science, Elsevier Science Publishers B.V., Amsterdam, The Netherlands, 150 pp., 1985.

Campbell Scientific: CS616 and CS625 water content reflectometers, Instruction manual, 2002–2006.

Collin, M. and Rasmuson, A.: A comparison of gas diffusivity models for unsaturated porous media, Soil Sci. Soc. Am. J., 52, 1559–1565, 1988.

Corre, M. D., Veldkamp, E., Arnold, J., and Wright, S. J.: Impact of elevated N input on N cycling and retention of soils under old-growth lowland and montane forests in Panama, Ecology, in press, 2010.

Crawley, M. J.: Statistical Computing, An Introduction to Data Analysis using S-Plus, John Wiley & Sons Ltd, Chichester, England, 761 pp., 2002.

Currie, J. A.: Gaseous diffusion in porous media. Part 3-Wet granular materials, British J. Appl. Phys., 12, 275–281, 1961.

Davidson, E. A. and Trumbore, S. E.: Gas diffusivity and production of CO_2 in deep soils of the eastern Amazon, Tellus, 47, 550–565, 1995.
Davidson, E. A., Ishida, F. Y., and Nepstad, D. C.: Effects of an experimental drought on soil emissions of carbon dioxide, methane, nitrous oxide, and nitric oxide in a moist tropical forest, Global Change Biol., 10, 718–730, 2004.
Davidson, E. A., Savage, K. E., Trumbore, S. E., and Borken, W.: Vertical partitioning of CO_2 production within a temperate forest soil, Global Change Biol., 12, 944–956, 2006.
DeJong, E. and Schappert, H. J. V.: Calculation of soil respiration and activity from CO_2 profiles in the soil, Soil Sci., 113, 328–333, 1972.
DeJong, E., Redmann, R. E., and Ripley, E. A.: A comparison of methods to measure soil respiration, Soil Sci., 127, 300–306, 1978.
Dörr, H. and Münnich, K. O.: ^{222}Rn flux and soil air concentration profiles in West-Germany. Soil ^{222}Rn as tracer for gas transport in the unsaturated soil zone, Tellus, 42B, 20–28, 1990.
Elberling, B.: Seasonal trends of soil CO_2 dynamics in a soil subject to freezing, J. Hydrol., 276, 159–175, 2003.
Fang, C. and Moncrieff, J. B.: A model for soil CO_2 production and transport 1: Model development, Agr. Forest Meteorol., 95, 225–236, 1999.
Fierer, N., Chadwick, O. A., and Trumbore, S. E.: Production of CO_2 in soil profiles of a California annual grassland, Ecosystems, 8, 412–429, 2005.
Gaudinski, J. B., Trumbore, S. E., Davidson, E. A., and Zheng, S.: Soil carbon cycling in a temperate forest: radiocarbon-based estimates of residence times, sequestration rates and partitioning of fluxes, Biogeochemistry, 51, 33–69, 2000.
Goldberg, S. D., Knorr, K.-H., and Gebauer, G.: N_2O concentration and isotope signature along profiles provide deeper insight into the fate of N_2O in soils, Isot. Environ. Healt. S., 44, 377–391, 2008.
Goldberg, S. D., Knorr, K.-H., Blodau, C., Lischeid, G., and Gebauer, G.: Impact of altering the water table height of an acidic fen on N_2O and NO fluxes and soil concentrations, Global Change Biol., 16, 220–233, 2010.
Hashimoto, S., Tanaka, N., Kume, T., Yoshifuji, N., Hotta, N., Tanaka, K., and Suzuki, M.: Seasonality of vertically partitioned soil CO_2 production in temperate and tropical forest, J. Forest Res., 12, 209–221, 2007.
Heincke, M. and Kaupenjohann, M.: Effects of soil solution on the dynamics of N_2O emissions: a review, Nutrient Cycling in Agro-Eosystems, 55, 133–157, 1999.

Hillel, D.: Environmental soil physics, Academic Press, San Diego, California, 771 pp., 1998.
Hirsch, A., Trumbore, S. E., and Goulden, M. L.: Direct measurement of the deep soil respiration accompanying seasonal thawing of a boreal forest soil, J. Geophys. Res., 108, 8221–8230, 2002.
IPCC: Climate Change 2007: The Physical Science Basis, Contribution of Working Group I to the Fourth Assessment Report of the Intergovernmental Panel on Climate Change, Cambridge University Press, Cambridge, UK and New York, USA, 2007.
Jassal, R., Black, A., Novak, M., Morgenstern, K., Nesic, Z., and Gaumont-Guay, D.: Relationship between soil CO_2 concentrations and forest-floor CO_2 effluxes, Agr. Forest Meteorol., 130, 176–192, 2005.
Jassal, R. S., Black, T. A., Drewitt, G. B., Novak, M. D., Gaumont-Guay, D., and Nesic, Z.: A model of the production and transport of CO_2 in soil: Predicting soil CO_2 concentrations and CO_2 efflux from a forest floor, Agr. For. Meteorol, 124, 219–236, 2004.
Kirkpatrick, S., Gelatt, C. D. J., and Vecchi, M. P.: Optimization by simulated annealing, Science, 220, 671–680, 1983.
Koehler, B., Corre, M. D., Veldkamp, E., and Sueta, J. P.: Chronic nitrogen addition causes a reduction in soil carbon dioxide efflux during the high stem-growth period in a tropical montane forest but no response from a tropical lowland forest on a decadal time scale, Biogeosciences, 6, 2973–2983, 2009a, http://www.biogeosciences.net/6/2973/2009/.
Koehler, B., Corre, M. D., Veldkamp, E., Wullaert, H., and Wright, S. J.: Immediate and long-term nitrogen oxide emissions from tropical forest soils exposed to elevated nitrogen input, Global Change Biol., 15, 2049–2066, 2009b.
Knorr, K.-H., Oosterwoud, M. R., and Blodau, C.: Experimental drought alters rates of soil respiration and methanogenesis but not carbon exchange in soil of a temperate fen, Soil Biol. Biochem., 40, 1781–1791, 2008a.
Knorr, K.-H., Glaser, B., and Blodau, C.: Fluxes and ^{13}C isotopic composition of dissolved carbon and pathways of methanogenesis in a fen soil exposed to experimental drought, Biogeosciences, 5, 1457–1473, 2008b, http://www.biogeosciences.net/5/1457/2008/.
Knorr, K.-H. and Blodau, C.: Impact of experimental drought and rewetting on redox transformations and methanogenesis in mesocosms of a northern fen soil, Soil Biol. Biochem., 41, 1187–1198, 2009.

Linn, D. M. and Doran, J. W.: Effect of water-filled pore space on carbon dioxide and nitrous oxide production in tilled and nontilled soils, Soil Sci. Soc. Am. J., 48, 1267–1272, 1984.
Loftfield, N., Flessa, H., Augustin, J., and Beese, F.: Automated gas chromatographic system for rapid analysis of the atmospheric trace gases methane, carbon dioxide, and nitrous oxide, J. Environ. Qual., 26, 560–564, 1997.
Luo, Y. and Zhou, X.: Soil respiration and the environment, Elsevier Academic Press, Burlington, San Diego and London, UK, 316 pp., 2006.
Millington, R. J. and Shearer, R. C.: Diffusion in aggregated porous media, Soil Sci., 111, 372–378, 1971.
Moldrup, P., Olesen, T., Schjønning, P., Yamaguchi, T., and Rolston, D. E.: Predicting the gas diffusion coefficient in undisturbed soil from soil water characteristics, Soil Sci. Soc. Am. J., 64, 94–100, 2000.
Pritchard, D. T. and Currie, J. A.: Diffusion coefficients of carbon-dioxide, nitrous-oxide, ethylene and methane in air and their measurement, J. Soil Sci., 33, 175–184, 1982.
Pylon Electronics: Using Pylon model 110A and 300A Lucas cells with the Pylon model AB-5, Instruction manual, 1989.
Radulovich, R., Solorzano, E., and Sollins, P.: Soil macropore size distribution from water breakthrough curves, Soil Sci. Soc. Am. J., 53, 556–559, 1989.
R Development Core Team: A language and environment for statistical computing. R Foundation for Statistical Computing, Vienna, http://www.R-project.org, 2009.
Richards, F. J.: A flexible growth function for empirical use, J. Exp. Bot., 10, 290–300, 1959.
Risk, D., Kellman, L., and Beltrami, H.: Carbon dioxide in soil profiles: Production and temperature dependence, Geophys. Res. Lett., 29, 012002, doi:10.1029/2001GL014002, 2002a.
Risk, D., Kellman, L., and Beltrami, H.: Soil CO_2 production and surface flux at four climate observatories in eastern Canada, Global Biogeochem. Cycles, 16, 1122, doi:1110.1029/2001GB001831, 2002b.
Risk, D., Kellman, L., and Beltrami, H.: A new method for in situ gas diffusivity measurement and applications in the monitoring of subsurface CO_2 production, J. Geophys. Res., 113, G02018, doi:02010.01029/02007JG000445, 2008.
Sander, R.: Compilation of Henry's Law Constants for inorganic and organic species of potential importance in environmental chemistry, http://www.mpch-mainz.mpg.de/~sander/res/henry.html, Max-Planck Institute of Chemistry, Mainz, 1999.
Sasaki, T., Gunji, Y., and Okuda, T.: Transient-diffusion measurement of radon in Japanese

soils from a mathematical viewpoint, J. Nucl. Sci. Technol., 43, 806–810, 2006.
Schwendenmann, L., Veldkamp, E., Brenes, T., O'Brien, J. J., and Mackensen, J.: Spatial and temporal variation in soil CO_2 efflux in an old-growth neotropical rain forest, La Selva, Costa Rica, Biogeochemistry, 64, 111–128, 2003.
Schwendenmann, L. and Veldkamp, E.: Long-term CO_2 production from deeply weathered soils of a tropical rain forest: evidence for a potential positive feedback to climate warming, Global Change Biol., 12, 1–16, 2006.
Šimůnek, J. and Suarez, D. L.: Modeling of carbon dioxide transport and production in soil 1. Model development, Water Resour. Res., 29, 487–497, 1993.
Šimůnek, J., Jarvis, N. J., van Genuchten, M. Th., and Gärdenäs, A.: Review and comparison of models for describing non-equilibrium and preferential flow and transport in the vadose zone, J. Hydrol., 272, 14–35, 2003.
Sotta E. D., Veldkamp, E., Schwendenmann, L., Guimaraes, B. R., Paixao, R. K., De Lourdes Ruivo, M., Da Costa, A. C. L., and Meir, P.: Effects of an induced drought on soil carbon dioxide (CO_2) efflux and soil CO_2 production in an Eastern Amazonian rainforest, Brazil, Global Change Biol., 13, 2218–2229, 2007.
Tse, F. C. and Sandall, O. C.: Diffusion coefficients for oxygen and carbon dioxide in water at 25˚C by unsteady state desorption from a quiescent liquid, Chem. Eng. Commun., 3, 147–153, 1979.
Veldkamp, E. and O'Brien, J. J.: Calibration of a frequency domain reflectometry sensor for humid tropical soils of volcanic origin, Soil Sci. Soc. Am. J., 64, 1549–1553, 2000.
Zehe, E. and Flühler, H.: Preferential transport of isoproturon at a plot scale and a field scale tile-drained site, J. Hydrol., 247, 100–115, 2001.
Zehe, E. and Sivapalan, M.: Threshold behaviour in hydrological systems as (human) geo-ecosystems: manifestations, controls, implications, Hydrol. Earth Syst. Sci., 13, 1273–1297, 2009,
http://www.hydrol-earth-syst-sci.net/13/1273/2009/.

Table 1. Mean (±SE) soil total porosity ($cm^3\,cm^{-3}$, n=3), its inter-aggregate (n=2) and air-filled fractions (% of total porosity, n=3) and radon production rates from air-dried and wet-season moist soil samples ($Bq\,kg^{-1}$ air-dry soil, n=3).

Depth (cm)	Porosity				Radon production	
	Total	Inter-aggregate	Air-filled during dry season	Air-filled during wet season	Air-dry soil	Wet-season moist soil
−5	0.78±0.02	29.8±7.9	56.0±0.5	40.5±1.1	2.8±0.6	4.4±0.9
−20	0.71±0.01	12.8±3.7	35.3±0.04	28.5±0.3	2.0±0.5	3.2±0.4
−40	0.62±0.01	11.2±5.0	20.0±3.0	17.1±2.2	1.8±0.4	2.5±0.5
−75	0.57±0.01	11.3±5.1	11.3±1.2	9.6±0.9	1.7±0.2	2.8±0.4
−125	0.57±0.02	5.4±0.4	11.1±3.6	9.6±3.2	1.6±0.3	2.4±0.3
−200	0.58±0.03	2.5±n.a.	11.3±4.6	10.6±4.2	1.3±0.3	2.5±0.6

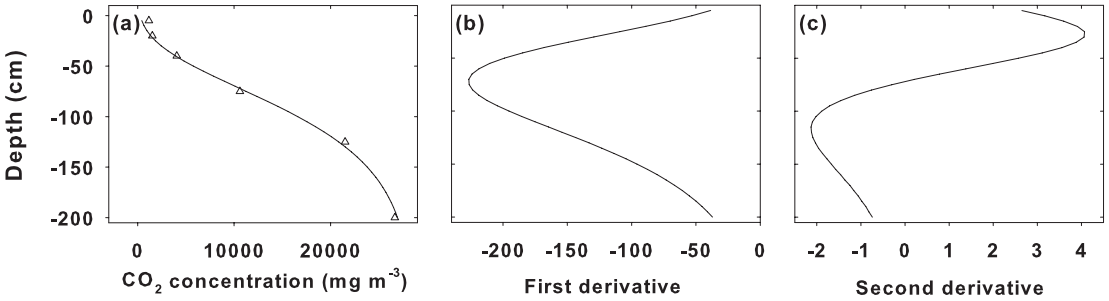

Fig. 1. **(a)** Sigmoidal function used to approximate profiles of CO_2 concentrations in soil air measured at our site (Δ, one exemplary profile) and its first **(b)** and second derivatives **(c)**, which are relevant terms in the soil-CO_2 profile method (Eq. 2).

BGD
7, 1489–1527, 2010

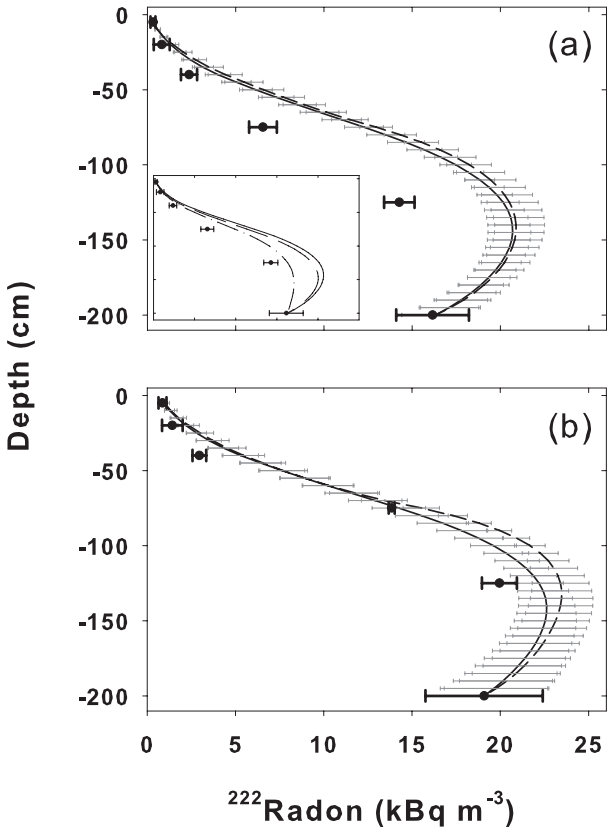

Fig. 2. Mean (±SE, n=3) measured Rn concentrations in soil air (•) during **(a)** dry and **(b)** wet seasons. The lines show the steady state profiles (±SE, n=3) simulated by a Rn mass balance model using the constrained inverse diffusion coefficients (D; —) and the empirical D (– –). The inset graph in (a) illustrates the sensitivity of the simulated Rn concentrations: The lines display the steady state modeled concentration profile using the inverse D (—), the response to a 20% increase in D (– –) and the response to a 20% reduction in the Rn production rates (– · –).

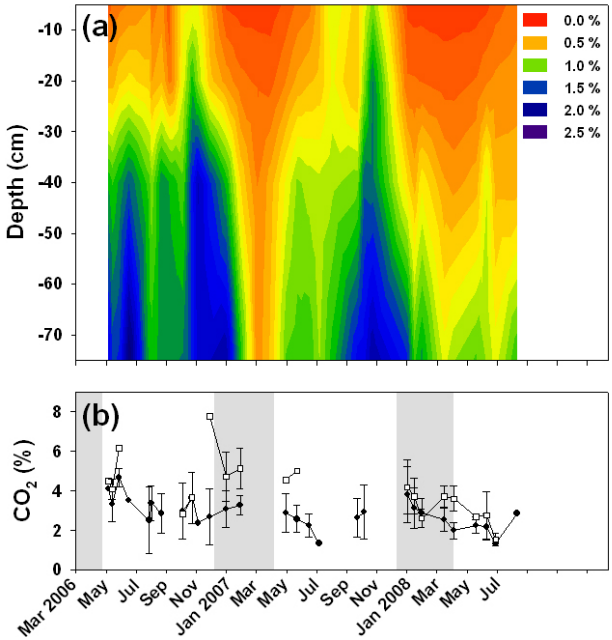

Fig. 3. Mean CO_2 concentrations in soil air (%) **(a)** interpolated between the four sampling depths in the top 0.75 m soil (n=3, SE range between 0.002 and 0.65%) and **(b)** for •=1.25 m and □=2 m depth (±SE, n=3). Grey shadings in (b) mark the dry seasons and missing wet season data are when high groundwater level restricted deep soil air sampling. Deep CO_2 concentrations are missing for the end of dry season 2007 due to analytical problems but top soil concentrations were determined.

BGD
7, 1489–1527, 2010

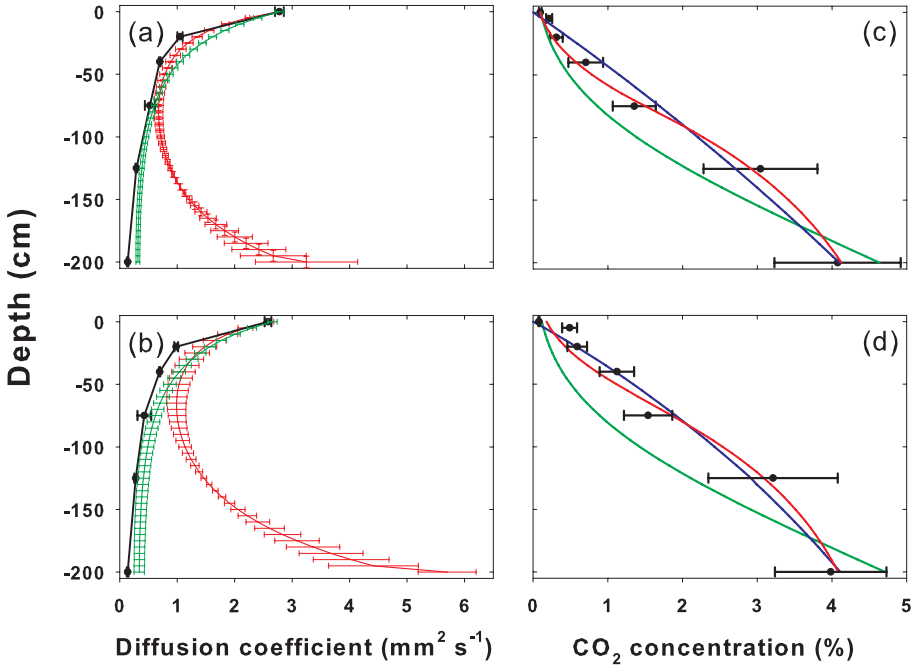

Fig. 4. Left panels: mean (±SE, n=3) dry **(a)** and wet season **(b)** empirical (•), unconstrained inverse (–) and constrained inverse (–) diffusion coefficients. Right panels: mean measured (•, ±SE, n=3) and interpolated (SE not shown for clarity of the figure) CO_2 concentrations in soil air during dry **(c)** and wet season **(d)** using the sigmoidal function with an unconstrained fit parameter choice (–), the sigmoidal function with a constrained fit parameter choice (–; see Sect. 2.2.2) and an exponential function (–).

BGD
7, 1489–1527, 2010

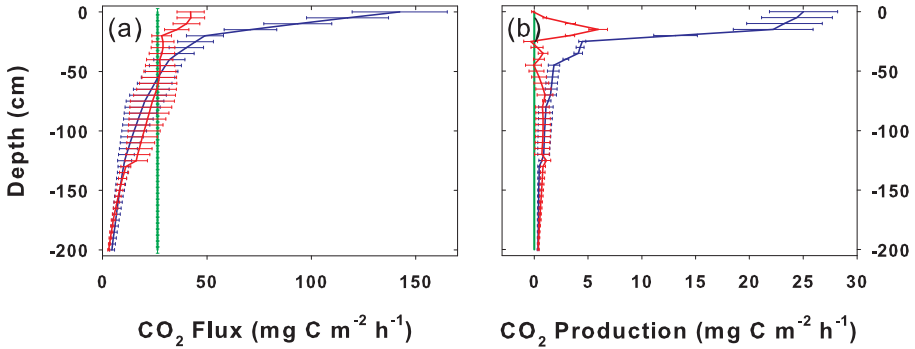

Fig. 5. Mean (±SE, n=3) soil CO_2 **(a)** fluxes and **(b)** production rates calculated with the soil-CO_2 profile method. The different solutions were obtained using the empirical diffusion coefficient (D) with a sigmoidal (–) and an exponential (–) function to interpolate between the measured CO_2 concentrations, and using the constrained inverse D which is based on the sigmoidal interpolation function (–).

BGD
7, 1489–1527, 2010

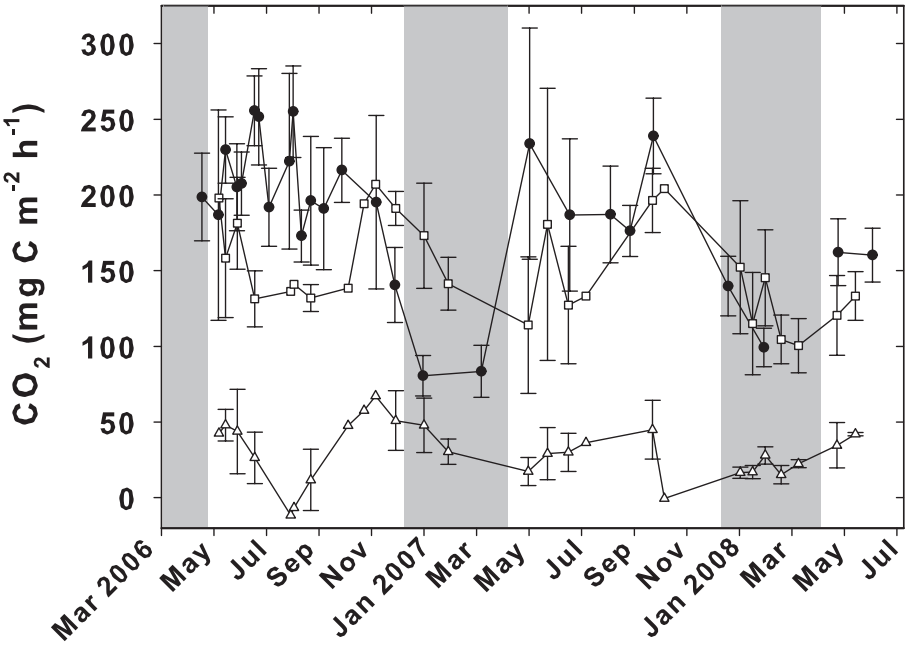

Fig. 6. Measured (•) and modeled mean soil CO_2 flux (±SE, n=3) using the empirical diffusion coefficients D with a sigmoidal (Δ) or exponential (□) function to approximate the measured CO_2 profiles.

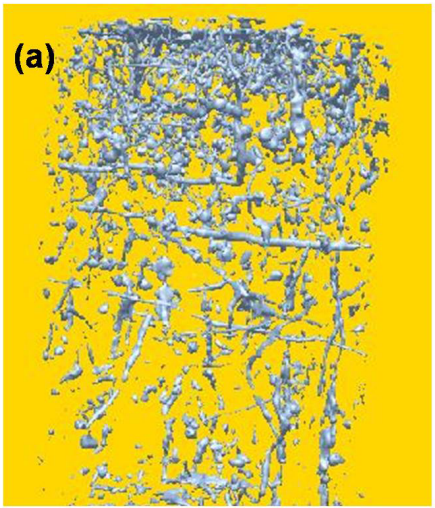

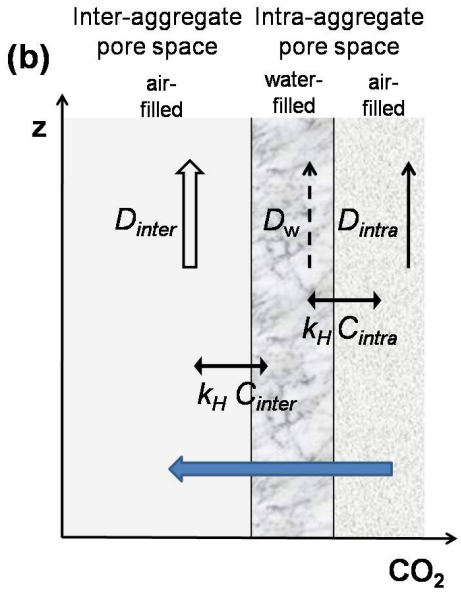

Fig. 7. **(a)** X-ray computed tomography scan of the inter-aggregate pores >2 mm (blue) in a Terra fusca soil. The image covers a depth of ~0.25 m. **(b)** Conceptual graph illustrating the CO_2 exchange at the interfaces between air- and water-filled pores. For simplicity, an equilibration according to Henry's law is assumed (C=CO_2 concentration, k_H=Henry's law constant). The different upward arrows illustrate that the diffusion coefficients D are larger in air-filled inter-aggregate (D_{inter}) than intra-aggregate pores (D_{intra}), and smallest in water-filled pores (D_w). This results in a CO_2 gradient and hence a net exchange flux which persists during steady state (blue arrow).